

Revisiting the “In-clustering” question in InGaN through the use of aberration-corrected electron microscopy below the knock-on threshold

Kamal H. Baloch, Aaron C. Johnston-Peck, Kim Kisslinger, Eric A. Stach, and Silvoja Gradečak

Citation: *Appl. Phys. Lett.* **102**, 191910 (2013); doi: 10.1063/1.4807122

View online: <http://dx.doi.org/10.1063/1.4807122>

View Table of Contents: <http://apl.aip.org/resource/1/APPLAB/v102/i19>

Published by the [American Institute of Physics](#).

Additional information on Appl. Phys. Lett.



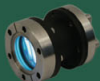



Journal Homepage: <http://apl.aip.org/>

Journal Information: http://apl.aip.org/about/about_the_journal

Top downloads: http://apl.aip.org/features/most_downloaded

Information for Authors: <http://apl.aip.org/authors>

ADVERTISEMENT

a sampling of our products		for surface and materials science	www. rbdinstruments .com	celebrating over 20 years of innovation
 deposition tools	 desorption systems	 sputter ion sources	 viewports	 usb picoammeters

Revisiting the “In-clustering” question in InGaN through the use of aberration-corrected electron microscopy below the knock-on threshold

Kamal H. Baloch,¹ Aaron C. Johnston-Peck,² Kim Kisslinger,² Eric A. Stach,^{2,a)} and Silvija Gradečak^{3,b)}

¹Research Laboratory of Electronics, Massachusetts Institute of Technology, Cambridge, Massachusetts 02139, USA

²Center for Functional Nanomaterials, Brookhaven National Laboratory, Upton, New York 11973, USA

³Department of Materials Science and Engineering, Massachusetts Institute of Technology, Cambridge, Massachusetts 02139, USA

(Received 23 April 2013; accepted 29 April 2013; published online 16 May 2013)

The high intensity of light emitted in $\text{In}_x\text{Ga}_{1-x}\text{N}/\text{GaN}$ heterostructures has been generally attributed to the formation of indium-rich clusters in $\text{In}_x\text{Ga}_{1-x}\text{N}$ quantum wells (QWs). However, there is significant disagreement about the existence of such clusters in as-grown $\text{In}_x\text{Ga}_{1-x}\text{N}$ QWs. We employ atomically resolved C_s -corrected scanning transmission electron microscopy and electron energy loss spectroscopy at 120 kV—which we demonstrate to be below the knock-on displacement threshold—and show that indium clustering is not present in as-grown $\text{In}_{0.22}\text{Ga}_{0.78}\text{N}$ QWs. This artifact-free, atomically resolved method can be employed for investigating compositional variations in other $\text{In}_x\text{Ga}_{1-x}\text{N}/\text{GaN}$ heterostructures. © 2013 AIP Publishing LLC. [<http://dx.doi.org/10.1063/1.4807122>]

Due to its unique optoelectronic properties, the semiconductor alloy InGaN finds increasing use in a wide range of applications, from light emitting diodes (LEDs),¹ to laser diodes,² photovoltaic solar cells,³ and solid-state bio-chemical sensors.⁴ Since the discovery of blue LEDs⁵—which have made phosphor-free white solid state lighting (SSL) a possibility⁶— $\text{In}_x\text{Ga}_{1-x}\text{N}$ ($0 \leq x \leq 1$) LED heterostructures composed of either single or multiple $\text{In}_x\text{Ga}_{1-x}\text{N}$ quantum wells (QWs) sandwiched between thin GaN layers have sparked tremendous interest. In particular, wavelength-tunable $\text{In}_x\text{Ga}_{1-x}\text{N}$ LEDs have been projected to increase the efficiency of SSL technology and, therefore, make a significant impact on energy consumption.^{7,8} However, despite the commercial success in recent years, InGaN/GaN LEDs have not reached their projected potential because their experimental efficiencies remain below theoretical predictions.⁹ In order to lower the cost and energy consumption, development of LEDs with efficiencies above 70% is required.⁸ Therefore, it is imperative to address unresolved fundamental scientific questions pertaining to the mechanisms and efficiency of the light emission in these heterostructures.

InGaN/GaN QWs are typically grown on a GaN buffer layer, which is grown on top of a sapphire or SiC substrate; because of the large lattice mismatch between the buffer layer and the substrate, InGaN layers contain a threading dislocation density (TDD) of 10^7 – 10^9 cm^{-2} or higher.¹ In spite of such high TDDs, InGaN based LEDs emit intense light, whereas presence of even a fraction of this TDD in other semiconductor LEDs completely quenches the light emission. It has been proposed that because InGaN is an alloy with a large miscibility gap, it can undergo spinodal decomposition resulting in the formation of In-rich clusters within the QWs.^{10,11} Whereas small-scale statistical fluctuations are

to be expected in any random ternary alloy, the In-clusters in InGaN were proposed to be large-scale (of 1–3 nm in size) and with significant compositional deviation from the nominal QW composition.¹² These In-rich clusters have been postulated to be critical to the observed high emission efficiency of InGaN, because they could act as sinks for electron-hole pairs where they recombine to emit light away from any light-quenching centers such as threading dislocations. However, the existence of the In-rich clusters is a topic of considerable debate. High-resolution transmission electron microscopy (HRTEM)¹⁰ and scanning transmission electron microscopy (STEM) studies combined with low-loss electron energy loss spectroscopy (EELS)¹² at accelerating voltages of 800 kV and 200 kV, respectively, suggested the existence of large-scale In-rich clusters adjacent to In-depleted regions in InGaN QWs. However, subsequent studies^{13,14} showed that no large-scale compositional fluctuations existed, beyond the small fluctuations expected in a random alloy such as InGaN. These authors suggested that exposure to a 200 kV or higher energy electron beam can cause irreversible irradiation damage in InGaN that could be misconstrued as spinodal decomposition. Thus, it was postulated that the reported In clustering was an artifact of TEM imaging and their existence in as-grown InGaN layers has since been questioned.

Although attempts have been made to minimize beam damage by investigating InGaN under low illumination current densities of 15 – 20 A cm^{-2} ,¹⁵ these studies have been conducted at accelerating voltages of $\geq 200 \text{ kV}$, which is presumably above the knock-on displacement damage threshold in these materials.¹⁶ Complementary techniques, such as atom probe tomography (APT), have also been employed to address the question of In clustering,^{14,17} but the inability of APT to attain atomic resolution in the lateral direction and lack of proper statistical sampling have rendered these studies inconclusive.¹⁸ In nearly the entire body of work

^{a)}Electronic mail: estach@bnl.gov

^{b)}Electronic mail: gradecak@mit.edu

pertaining to In clustering, TEM investigations were done by employing conventional (non-aberration corrected) TEMs. For these instruments, it is not possible to obtain atomic resolution at lower accelerating voltages and thus it has been difficult to conclusively rule out knock-on displacement damage as the origin of the observed large-scale In clusters. This debate on the existence of In clusters is further complicated by the fact that studies by different groups used samples grown under different conditions, and is known that variations in growth conditions and composition, x , of the $\text{In}_x\text{Ga}_{1-x}\text{N}$ alloy can influence its structural, electronic, and optical properties.^{19,20} In this work, we employ atomically resolved aberration (C_s)-corrected S/TEM operated at 80 kV and 120 kV for structural and electronic characterization of InGaN QWs samples and demonstrate that these operational conditions are below the knock-on displacement threshold. Critically, the samples we are investigating here are from the same region of the same InGaN QWs wafer used in Ref. 13, the study that first questioned the existence of In-rich clusters.

The InGaN/GaN samples were grown by metalorganic vapor phase epitaxy and were composed of 10 $\text{In}_{0.22}\text{Ga}_{0.78}\text{N}$ 2.8 nm-thick QWs separated by 7.2 nm-thick GaN barriers. The thickness of the QWs and their nominal composition were calculated by x-ray reflectivity and x-ray diffraction.¹³ Room temperature cathodoluminescence of the wafer showed a high intensity peak centered at 508 nm consistent with the nominal In composition of 22%.^{21,22} We have independently verified the nominal composition by APT measurements (not described herein). Electron transparent TEM films were prepared from the parent wafer using a FEI Helios 600 dual beam focused ion beam (FIB) operated at 30 kV. A final cleaning step using a FIB voltage of 5 kV was also performed. The amorphized surface layer—an inevitable consequence of gallium ion (Ga^{2+}) implantation during FIB milling—was removed by a wet-chemical etch at room temperature using 14% weight/volume solution of potassium hydroxide (KOH) for 3–5 min. Finally, to remove any residue of the wet-etch, samples were cleaned in a low power 75% argon and 25% oxygen plasma for 20 min. HRTEM imaging of our samples was carried out in an image-corrected FEI Titan 80–300 TEM operated at 80 kV, while STEM and EELS studies were performed using a probe-corrected Hitachi HD-2700C operated at 120 kV.

The resulting TEM samples were <20 nm thick, as measured by EELS, and have minimal surface damage (Figure 1). If present, contrast from In-rich regions in InGaN can be observed using high-angle annular dark-field (HAADF) STEM due to the significant difference in the atomic numbers of In ($Z=49$) and Ga ($Z=31$).²³ Additionally, C_s -correction of the electron probe makes atomically resolved STEM imaging possible, even at accelerating voltages lower than 200 kV. To confirm that the use of low-voltage STEM mitigates the effects of beam damage, we obtained STEM data as a function of the exposure time using an electron beam with the spot size of ~ 1 Å and a typical current density of <0.9 A cm^{-2} . These parameters are an order of magnitude smaller compared to previously reported HAADF-STEM and EELS¹⁰ (the beam spot size of 0.14 nm and ~ 1 nm, respectively) or HRTEM¹³ (current density of 35 A cm^{-2}) studies. Recently, a C_s -TEM study²⁴ and a

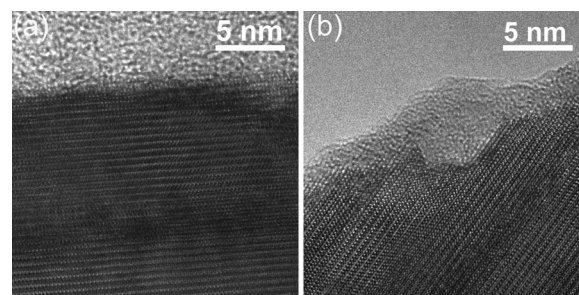


FIG. 1. C_s -HRTEM micrographs of the investigated InGaN QWs sample acquired at an accelerating voltage of 80 kV before and after surface cleaning. (a) Image showing the top of the sample prepared by FIB milling. The contrast variations correspond to surface damage caused by ion-milling. (b) Approximately the same region as shown in (a) after a chemical etch in KOH followed by plasma cleaning. This protocol is effective in removing surface amorphization caused by Ga implantation during sample preparation by FIB.

C_s -STEM study²⁵ were performed using a dose on the same order as in our experiments; however, these studies were conducted at 300 kV and 200 kV, respectively, which are above the knock-on threshold for the InGaN alloy. Figure 2(a) presents a C_s -STEM HAADF micrograph acquired at 120 kV shortly after aligning the electron microscope ($t=0$ min) in a different sample location. It can be seen that there are no large-scale contrast variations—as would be expected for large-scale In-rich clusters—in the InGaN QWs. By comparing Figure 2(a) with an image acquired after 16 min of continuous exposure (Figure 2(b)), no change in contrast with exposure time was observed. Together with a higher magnification, lattice resolved STEM image of one of the QWs (Figure 2(c)), these results confirm that there are no large-scale compositional fluctuations inside the QWs or significant electron beam damage after exposure of more than 16 min.

We note that the small variations in contrast apparent in Figure 2 can be attributed to residual surface amorphization that was not removed by the KOH wet-etch and is a consequence of FIB milling, as confirmed by a HRTEM focal series reconstruction shown in supplementary information.³⁰ We repeated the same experiments on three different sets of samples prepared from the same wafer and using the same protocol described above. Several sets of time series acquired on each TEM sample gave consistent results. Furthermore, control experiments were performed by operating the C_s -corrected HRTEM at accelerating voltages of 200 kV and 300 kV and these showed significant electron beam damage to our samples, which was manifested as contrast variations in HRTEM images with prolonged exposure time. However, C_s -HRTEM images acquired at 80 kV and diffraction contrast imaging done at 120 kV showed no significant electron beam damage. Since the illumination current density is significantly lower in C_s -STEM mode, we can conclude that our approach of acquiring STEM data at 120 kV does not cause significant beam damage in the investigated samples.

In addition to HAADF STEM imaging, another method to detect In segregation is by measuring the low-loss region of the EELS spectrum.¹² After the zero-loss peak (ZLP), the most intense and easily identifiable peak in the low-loss EELS spectrum corresponds to the bulk plasmon resonance. The energy of the plasmon peak (E_p) is composition-

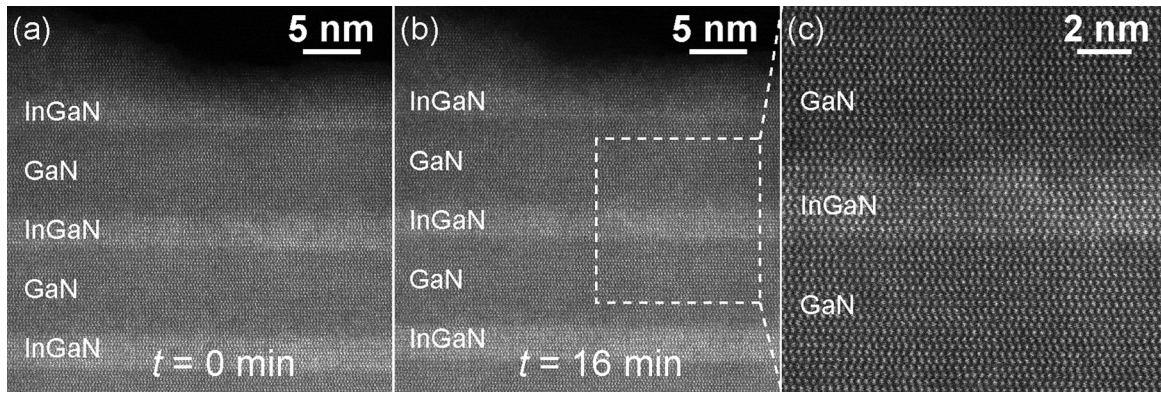


FIG. 2. Time-series of the top three InGaN QWs separated by GaN barriers acquired by C-S-STEM at 120 kV at (a) $t = 0$ min and (b) $t = 16$ min. (c) Higher magnification image of the middle QW showing that there are no In-rich clusters present in the InGaN QWs. Together, these images confirm that there is no beam induced damage at 120 kV.

dependent and is, therefore, characteristic of the alloy composition.²⁶ However, the exact dependence of E_p of a ternary alloy on elemental composition, x , is not well understood. Some studies have suggested a linear dependence of E_p on x ,²⁷ while some have suggested a variation or “bowing” of E_p consistent with Vergard’s Law.²⁶ Thus, for $\text{In}_x\text{Ga}_{1-x}\text{N}$, the plasmon energy can be described as

$$E_p^{\text{InGaN}} = x E_p^{\text{InN}} + (1 - x)E_p^{\text{GaN}} - b_{\text{plasmon}}x(1 - x), \quad (1)$$

where E_p^{InGaN} , E_p^{InN} , and E_p^{GaN} are the plasmon energies of the respective materials and b_{plasmon} is the bowing parameter. While $E_p^{\text{InN}} = 15.7$ eV (Ref. 28) and $E_p^{\text{GaN}} = 19.15$ eV are well documented for thin films,²⁹ there is no agreement on the value of b_{plasmon} . By using the nominal In composition $x = 0.22$ and experimentally obtained average $E_p^{\text{GaN}} = 19.125$ eV and $E_p^{\text{InGaN}} = 18.810$ eV (reported later in this manuscript), we calculate $b_{\text{plasmon}} = -2.55$ eV (see supplementary information)³⁰ and this value can be used to calculate the alloy composition for each measured E_p^{InGaN} value. In this work, we rely on the change in E_p measured along a QW to ascertain the existence or absence of In-clusters. The measured variation in E_p is used to calculate the corresponding change in In composition, Δx , by assuming both a linear as well as a bowing relationship between E_p and x .

Low-loss EELS data were acquired by scanning a focused 120 kV electron beam along several GaN and InGaN layers. The data have an energy dispersion of 0.1 eV/channel and an energy resolution of <600 meV, determined from the full width at half maximum of the ZLP. To check the validity and reproducibility of the low-loss EELS data, line scans were first acquired along two different GaN barrier regions in steps of 0.3 nm, and were analyzed individually to identify the position of E_p . For each acquired spectrum, the tail of the ZLP was first removed using a Fourier-log routine, and care was taken to ensure that low-energy features were not lost in the process.²⁶ A representative ZLP-subtracted EELS spectrum is shown in Figure S3 (supplementary information). E_p was extracted from the spectra and plotted as a function of the relative position along the line scan (Figure 3). This process was then repeated for two different InGaN QWs and also plotted in Figure 3. The EELS data were acquired in regions that are sufficiently away from each other because the

build-up of carbon contamination during data acquisition over an extended period of time can lower the signal-to-noise ratio.

We measure E_p^{GaN} to be 19.10 eV and 19.15 eV for the two GaN barriers identified in Figure 3. It is to be noted that E_p^{GaN} remains constant for each GaN barrier, thereby confirming the expected compositional uniformity in GaN. The difference in E_p^{GaN} for the two different GaN barriers is within the error of measurement (± 0.1 eV). These measured values are in agreement with the literature, again confirming the validity and reproducibility of our technique. By following the same procedure, E_p^{InGaN} was measured at each scan point for the two InGaN QWs identified in Figure 3. The average value of E_p^{InGaN} for QW 1, identified as InGaN 1 in Figure 3, is 18.84 eV and for QW 2, identified as InGaN 2 in Figure 3, is 18.78 eV. In composition in different QWs can be different even when grown under identical conditions; thus, the average E_p^{InGaN} is expected to be different in two different QWs. However, the variation of E_p^{InGaN} within individual QWs merits a more detailed discussion. It can be seen from Figure 3 that data points spanning a few-nm correspond to $E_p^{\text{InGaN}} = (18.8\text{--}18.9)$ eV in QW 1 and similarly $E_p^{\text{InGaN}} = (18.75\text{--}18.85)$ eV in QW 2. To investigate whether the observed ~ 0.1 eV changes in E_p^{InGaN} can be ascribed to

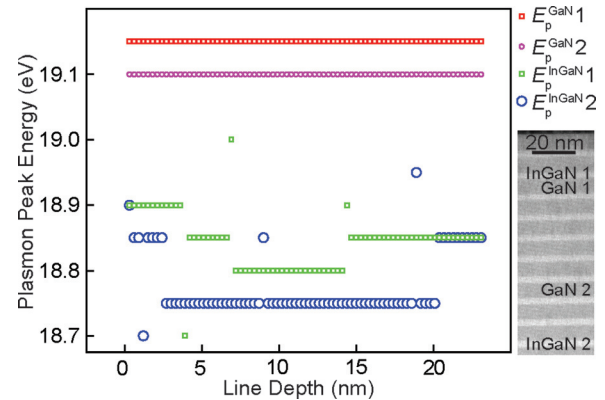


FIG. 3. E_p^{GaN} and E_p^{InGaN} extracted from low-loss EELS data plotted as a function of scan position. Lack of variations in E_p^{GaN} 1 and E_p^{GaN} 2, corresponding to extracted E_p values of two different GaN barriers, along the scan direction confirm the validity and reproducibility of our methodology. Low-loss EELS line scans in the two QW regions show that the compositional variation corresponding to the shift in $\Delta E_p^{\text{InGaN}}$ is $<5.4\%$.

large scale In clustering, we calculate the compositional change Δx that would correspond to these variations (see supplementary information for more details). For QW1 (QW2), we find $\Delta x = 2.4\%$ or 5.2% ($\Delta x = 3.0\%$ or 5.4%), depending upon the assumptions of linearity or bowing of E_p with x , respectively. Such small variations are due to the statistical fluctuations of a random alloy and are compositionally too small to be attributed to the existence of large scale In-rich clusters.¹² Furthermore, no additional secondary bulk plasmon peaks were observed in the EELS spectra collected along the InGa_N QWs. Taken together, the EELS results are consistent with the STEM images from Figure 2, and imply that there is no large-scale In-clustering in either of the InGa_N QWs.

In summary, we have employed C_S-corrected STEM imaging and EELS measurements below the knock-on threshold to determine the compositional variation in InGa_N QWs. By combining careful sample preparation and low-voltage imaging, we have demonstrated the ability to characterize InGa_N MQWs without introducing electron beam artifacts. The samples studied were the same as those investigated by Smeeton *et al.*¹³ and we confirm their observation that no gross-scale compositional fluctuations are present in those samples. However, it is possible that other samples—having different compositions or different processing parameters—may in fact show compositional fluctuations. While our results cannot imply that large-scale compositional fluctuations do not occur in any In_xGa_{1-x}N sample, we clearly demonstrate that the samples under investigation do not contain large-scale compositional fluctuations, and, importantly, they are apparently not critical for strong light emission. Finally, we have also established a systematic methodology to investigate this question in other In_xGa_{1-x}N heterostructures. It is anticipated that this approach can be used to clarify the role of structural inhomogeneities in light emission in these systems.

The authors acknowledge Professor Colin J. Humphreys for providing the samples and Dr. Dong Su and Professor Marc Baldo for useful discussions. This work was supported by The Center for Excitonics, an Energy Frontier Research Center funded by the U.S. Department of Energy, Office of Science, Office of Basic Energy Sciences under Award No. DE-SC0001088. The research at the Center for Functional Nanomaterials, Brookhaven National Laboratory was supported by the U.S. Department of Energy, Office of Basic Energy Sciences, under Contract No. DE-AC02-98CH10886. The authors acknowledge access to Shared Experimental Facilities provided by the MIT Center for Materials Science Engineering supported in part by the MRSEC Program of the National Science Foundation under Award No. DMR-0213282.

- ¹S. Nakamura, *Science* **281**(5379), 956–961 (1998).
- ²S. Nakamura, M. Senoh, S. Nagahama, N. Iwasa, T. Yamada, T. Matsushita, H. Kiyoku, and Y. Sugimoto, *Jpn. J. Appl. Phys., Part 2* **35**(1B), L74–L76 (1996).
- ³N. G. Toledo and U. K. Mishra, *J. Appl. Phys.* **111**, 114505 (2012).
- ⁴B. Lubbers, G. Kittler, P. Ort, S. Linkohr, D. Wegener, B. Baur, M. Gebinoga, F. Weise, M. Eickhoff, S. Maroldt, A. Schober, and O. Ambacher, *Phys. Status Solidi C* **5**(6), 2361–2363 (2008).
- ⁵S. Nakamura, N. Iwasa, and S. Nagahama, *Jpn. J. Appl. Phys., Part 2* **32**(3A), L338–L341 (1993).
- ⁶M. Yamada, Y. Narukawa, and T. Mukai, *Jpn. J. Appl. Phys., Part 2* **41**(3A), L246–L248 (2002).
- ⁷M. P. Vittiow and P. W. Brittenham, *Basic Research Needs for Solid-State Lighting: Report of the Basic Energy Sciences Workshop on Solid-State Lighting* (Department of Energy, 2006).
- ⁸J. Y. Tsao, M. E. Coltrin, M. H. Crawford, and J. A. Simmons, *Proc. IEEE* **98**(7), 1162–1179 (2010).
- ⁹J. M. Phillips, M. E. Coltrin, M. H. Crawford, A. J. Fischer, M. R. Krames, R. Mueller-Mach, G. O. Mueller, Y. Ohno, L. E. S. Rohwer, J. A. Simmons, and J. Y. Tsao, *Laser Photonics Rev.* **1**(4), 307–333 (2007).
- ¹⁰C. Kisielowski, Z. Liliental-Weber, and S. Nakamura, *Jpn. J. Appl. Phys., Part 1* **36**(11), 6932–6936 (1997).
- ¹¹Y. Narukawa, Y. Kawakami, M. Funato, S. Fujita, S. Fujita, and S. Nakamura, *Appl. Phys. Lett.* **70**(8), 981–983 (1997).
- ¹²J. R. Jinschek, R. Erni, N. F. Gardner, A. Y. Kim, and C. Kisielowski, *Solid State Commun.* **137**(4), 230–234 (2006).
- ¹³T. M. Smeeton, M. J. Kappers, J. S. Barnard, M. E. Vickers, and C. J. Humphreys, *Appl. Phys. Lett.* **83**(26), 5419–5421 (2003).
- ¹⁴S. E. Bennett, D. W. Saxey, M. J. Kappers, J. S. Barnard, C. J. Humphreys, G. D. W. Smith, and R. A. Oliver, *Appl. Phys. Lett.* **99**, 021906 (2011).
- ¹⁵V. B. Ozdol, C. T. Koch, and P. A. van Aken, *J. Appl. Phys.* **108**, 056103 (2010).
- ¹⁶R. F. Egerton, P. Li, and M. Malac, *Micron* **35**(6), 399–409 (2004).
- ¹⁷M. J. Galtrey, R. A. Oliver, M. J. Kappers, C. J. Humphreys, D. J. Stokes, P. H. Clifton, and A. Cerezo, *Appl. Phys. Lett.* **90**, 061903 (2007).
- ¹⁸C. Kisielowski and T. P. Bartel, *Appl. Phys. Lett.* **91**, 176101 (2007).
- ¹⁹F. K. Yam and Z. Hassan, *Superlattices Microstruct.* **43**, 1–23 (2008).
- ²⁰V. N. Jmerik, A. M. Mizerov, T. V. Shubina, D. S. Plotnikov, M. V. Zamoryanskaya, M. A. Yagovkina, Y. V. Domracheva, A. A. Sitnikova, and S. V. Ivanov, *Semiconductors* **42**(5), 616–623 (2008).
- ²¹K. P. O'Donnell, I. Fernandez-Torrente, P. R. Edwards, and R. W. Martin, *J. Cryst. Growth* **269**(1), 100–105 (2004).
- ²²P. G. Moses and C. G. Van de Walle, *Appl. Phys. Lett.* **96**, 021908 (2010).
- ²³A. Rosenauer, T. Mehrtens, K. Muller, K. Gries, M. Schowalter, P. V. Satyam, S. Bley, C. Tessarek, D. Hommel, K. Sebal, M. Seyfried, J. Gutowski, A. Avramescu, K. Engl, and S. Lutgen, *Ultramicroscopy* **111**(8), 1316–1327 (2011).
- ²⁴T. Schulz, T. Remmele, T. Markurt, M. Korytov, and M. Albrecht, *J. Appl. Phys.* **112**(3), 033106 (2012).
- ²⁵A. B. Yankovich, A. V. Kvit, X. Li, F. Zhang, V. Avrutin, H. Y. Liu, N. Izyumskaya, Ü. Özgür, H. Morkoç, and P. M. Voyles, in *MRS Proceedings* (2012), Vol. 1432.
- ²⁶A. Eljarrat, S. Estrade, Z. Gacevic, S. Fernandez-Garrido, E. Calleja, C. Magen, and F. Peiro, *Microsc. Microanal.* **18**(5), 1143–1154 (2012).
- ²⁷J. Palisaitis, C. L. Hsiao, M. Junaid, M. Y. Xie, V. Darakchieva, J. F. Carlin, N. Grandjean, J. Birch, L. Hultman, and P. O. A. Persson, *Phys. Status Solidi (RRL)* **5**(2), 50–52 (2011).
- ²⁸P. Specht, J. C. Ho, X. Xu, R. Armitage, E. R. Weber, R. Erni, and C. Kisielowski, *Solid State Commun.* **135**(5), 340–344 (2005).
- ²⁹M. Bosman, L. J. Tang, J. D. Ye, S. T. Tan, Y. Zhang, and V. J. Keast, *Appl. Phys. Lett.* **95**, 101110 (2009).
- ³⁰See supplementary material at <http://dx.doi.org/10.1063/1.4807122> for focal series reconstruction and low-loss electron energy loss spectroscopy analysis.